Effects of alumina on the stability of ferrite–calcium sinter with dicalcium silicate

***I. N. Pyagay**, Dr. Eng., Senior Researcher[1], Director of Scientific Center "The problems of processing of mineral and technogenic resources", e-mail: igor-pya@yandex.ru;*
***A. B. Lebedev**, Cand. Eng., Researcher[1], Scientific Center "The problems of processing of mineral and technogenic resources", e-mail: 2799957@mail.ru*

[1] Empress Catherine II St. Petersburg Mining University (St. Petersburg, Russia)

Laboratorial production of agglomerate with basicity CaO/SiO_2 = 1.3-1.5 is accompanied by its spontaneous friability, what leads to forming of visible cracks in agglomerate. When studying the influence of these sintering parameters on agglomerate strength, it is necessary to take into account content of not assimilated calcium oxides in sinter. Strength binding of agglomerate is formed on the base of calcium ferrites. Investigations were conducted on aluminium oxide of PA grade, Fe_2O_3, $CaCO_3$ of PA grade, aqueous silicic acid of P grade. Stability of sinters for above-mentioned systems was determined visually and using high-frequency method. In the first case the high-temperature Tamman furnace is used, where briquetted samples are put in a platinum cup and they are heated up to the temperature 1300 °C. Then, after 5 minutes holding for homogenization, the samples are cooled slowly together with the furnace to the temperature 500 °C. To determine the temperature of β→γ transition of dicalcium silicate, dielectric permeability is measured; it reacts on structural changes which cause variation of density. The boundary of sinters stability is situated along the line which is close to galenite. The part of aluminium oxide interacts with dicalcium ferrite and forms solid solutions together with complete Fe replacement by Al in dicalcium ferrite. Stable sinters are characterized by monotonous variation of dielectric losses and capacity in the conditions of complete dicalcium silicate binding by aluminium oxide. It was established that monocalcium ferrite does not form new compounds with aluminium oxide, which completely interacts with dicalcium silicate. The stable samples of the system $CaFe_2O_4$–Ca_2SiO_4–Al_2O_3 are characterized by increase of alumosilicate amount and decrease of dicalcium silicate amount. When Ca_2SiO_4 content decreases from 45 % to 28 %, the temperature reduces from 390–405 °C до 265–275 °C. Agglomerate containing 7 % of alumina practically does not contain free calcium oxide, what removes the cause of stresses appearing in the sinter. As a result of stabilization of ferrite-calcium sinter via replacement of silicon module by aluminium one, compression strength value increases up to 235 daN for a briquette.

Key words: pellets, agglomerate, sinter, heat treatment, alumina effect, stabilization of ferrite-calcium sinter, dicalcium silicate.
DOI: 10.17580/cisisr.2023.01.02

Introduction

Agglomerate makes more than 60 % of blast furnace charge materials in Russian Federation, thereby the problem of its quality improvement is rather actual. Production of fluxed agglomerate can be characterized by its local strength minimum within the basicity interval 1.3 – 1.7 [1-3].

It is explained by several causes: polymorphism of dicalcium silicate with increase of volume of substances, forming of sinter stress state during cooling, non-uniformity of elements distribution in sinter etc. Dicalcium silicate can be revealed together with cracks, which rose as a result of appearance of local internal stresses, during microscopic analysis [4-6].

The work [7] testifies that addition of aluminium and magnesium oxides to sinter allows to neutralize the effect of this factor and to be the method for increase of agglomerated raw material strength. In this case, several researches [8-10] stated possibility of manufacture of high-strength agglomerate based on its binding with prevalence of calcium ferrites.

Absence of non-assimilated flux in agglomerate structure is considered as the condition of production of high-quality agglomerate. Possibility of maximal assimilation of calcium oxide in composition of agglomerate sinter for dual-component compounds can be determined via the formula (1):

$$CaO_{max} \le 0.11\ Fe^{2+} + 0.35\ Fe^{3+} + 1.06\ TiO_2 + 1.64\ Al_2O_3 + 2.82\ SiO_2 \quad (1)$$

where CaO_{max} – maximal allowable content of calcium oxide in composition of sintered agglomerate; Fe_2O_3, Fe_3O_4, TiO_2, Al_2O_3, SiO_2 – content of oxides in the same agglomerate, %.

Bauxite which is used for laboratorial investigation contains (%):15.8 $Fe_{tot.}$; 2.6 FeO, 2.2 CaO; 4.7 SiO_2; 55.1 Al_2O_3; 1.5 TiO_2, respectively, maximal amount of calcium oxide can make:

$$CaO_{max} = 0.11 \cdot 2.1 + 0.852 \cdot 13.7 + 1.058 \cdot 1.5 + 1.645 \cdot 55.1 + 2.816 \cdot 4.7 = 110.55 \quad (2)$$

SiO_2 content 0.3-0.4 % in sintered agglomerate with basicity about 1.4 allows to obtain sinter with completely assimilated calcium oxide in a dual-component compound. To provide complete assimilation of calcium oxide during agglomerate sintering, when this agglomerate contains alumina with basicity 6-8, complete involvement of calcium oxide in chemical compound is required [10-12].

Maximal assimilation of calcium oxide in agglomerate from iron ore concentrate with the following composition (%): 60 Fe; 5 SiO_2; 2 Al_2O_3; 1 TiO_2 etc. can be expressed via the equation (3):

$$CaO = 0.11 + 0.852 \cdot 50 + 1.058 \cdot 1.0 + 1.645 \cdot 2.0 + + 2.816 \cdot 5 = 34.5 \quad (3)$$

The conducted calculations display only potential possibility, not concrete conditions of complete flux assimilation in agglomerate composition. These conditions are determined by technological parameters of sintering (optimal fuel consumption, height of charge material layer, introduction of additives having the effect on the temperature level of sinter forming) [13, 14].

When studying the influence of the above-mentioned sintering parameters on agglomerate strength, it is necessary to take into account content of not assimilated calcium oxides in sinter, what will further determine integrity of the structure during storage with possibility of medium humidity variation [15].

Strengthening agglomerate binding is forming on the base of calcium ferrites. Calcium ferrites can stabilize less amount of mixture in comparison with Ca_2SiO_4, which occupies up to 25 % of total volume, in the conditions of sintering at the temperature not higher than softening temperature. In this case sinter should have sufficient strength and stability to scattering, what is provided by sinter stability after its complete assimilation of calcium oxide. Forming of new phases, having the strengthening effect of the system in general, is possible during structure forming [16-18]. Thereby examination of Al_2O_3 influence on stability of ferrite-calcium sinter, which contains Ca_2SiO_4, is considered as a priority task of this research.

Examination of mineral forming during sintering of agglomerate on the base of ferrite-calcium and dicalcium silicate due to introduction of varying alumina additive, as well as development of technological solutions for increase of sinter strength on this base, are the aim of this work. Such goal setting is caused by absence of any information in the technical literature at present time about the mechanism of aluminium oxide influence on stability of ferrite-calcium sinter. It just stipulates the research novelty.

Materials and methods

Preliminarily prepared calcium ferrites, dicalcium silicate and aluminium oxides of PA grade are the initial materials for manufacture of samples. Calcium ferrite and silicate are obtained from the following chemical substances: Fe_2O_3 – for ferrites, $CaCO_3$ –from PA grade, aqueous silicic acid of P grade.

The mixture of Fe oxide, calcium carbonate and aqueous silicic acid is composed in correspondence with the stoichiometric compositions of calcium ferrites or dicalcium silicate. Each mixture was stirred in a mill during two hours in alcohol presence to provide homogenization; this mill is filled for one third by metal balls of different diameter. Briquettes with diameter 20 and h=10 are manufactured from the mixture which was dried at 100 °C. Calcium ferrites and dicalcium silicate are forming during sintering [19-21].

Stability of sinters of above-mentioned systems is determined visually using high-frequency method. In the first case high-temperature Tamman furnace is used, where briquetted samples are put in a platinum cup and they are heated up to the temperature 1300 °C. Then, after 5 minutes holding for homogenization, the samples are cooled slowly together with the furnace to the temperature 500 °C. Microstructure of non-stable sinter (60 % Fe_2O_3 – 37 % Ca_2SiO_4 – 3 % Al_2O_3) and stable sinter (60 % Fe_2O_3 – 25 % Ca_2SiO_4 – 15 % Al_2O_3) is presented on the **Fig. 1**.

The second technique is used to determine the temperature of β→γ transition of dicalcium silicate, which is based on measurement of electric parameters of substance in high-frequency field [22-24].

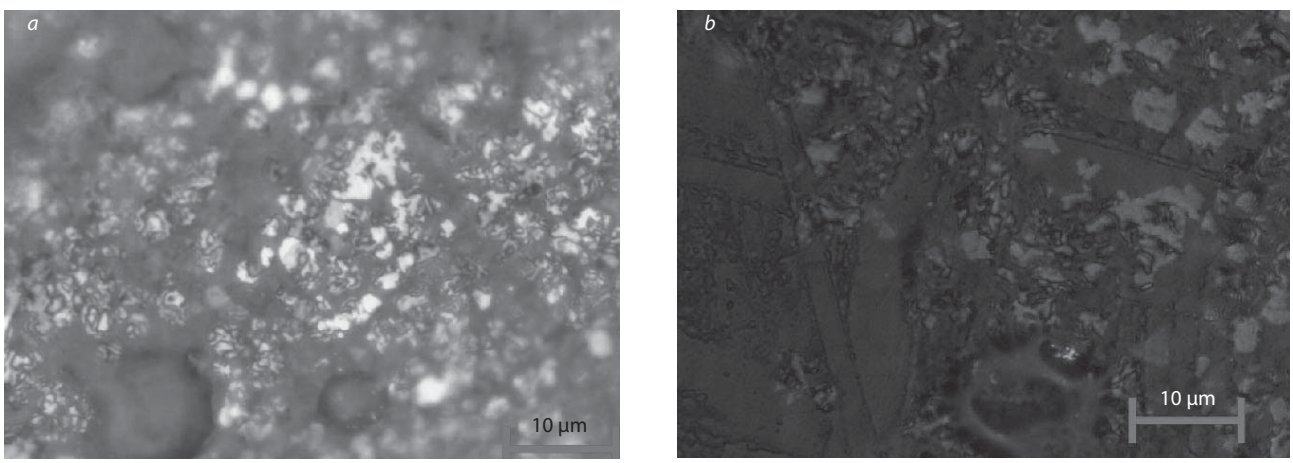

Fig. 1. Microstructure of sinter of calcium ferrite and dicalcium silicate together with alumina – non-stable (*a*) and stable (*b*) [these results were obtained by the authors]

Dicalcium silicate can be related to the olivine row of island structures, where silicon oxide tetrahedrons (SiO_4)-4 are connected together by cations. The mechanism of polymorphic transformations is connected with transition of atoms in combination with definite turn of tetrahedrons. Variation of the temperature leads to variation of ions polarization, which finalizes in dimensional redistribution of compactly packed oxygen ions [25-27].

Dielectric permeability characterizes ability of dielectric particles to orient or change their location after alternation of the field sign at preset frequency and temperature. That's why dielectric permeability reacts on structural changes in the same way as variation of the number of polarizing particles per volume unit, which causes corresponding sample density variation (it decreases by 10-12 % at β→γ transition of dicalcium silicate) [28-30].

Measurements of dielectric permeability and dielectric losses are not interchangeable, but they reflect different parts of the general event.

The principle is based on registration on variation of condenser capacity, where the examined substance is a dielectric (dicalcium silicate is included in its composition), as well as on variation of dielectric losses in oscillating circuit.

A flat-bottomed platinum cup with 12 mm diameter, where the examined briquette is placed, is a lower electrode of the measuring condenser. The second electrode in the form of platinum disc is placed just near to the briquette using special fixer from the top. The temperature is measured by platinum/platinum-rhodium thermocouple, which is connected with briquette from bottom through the hole of the lower electrode cup. The scheme of this unit with the high-temperature measuring cell is presented on the **Fig. 2**.

The particles during polymorphic transformation should overcome any energetic barriers. At the same time, part of them can be classified both to old and new lattices (monoclinic β–form, rhombic γ–form), thereby the transformation period should be characterized as a peak on polytherms of electric properties. The curves of capacity (C) and dielectric loss (ε) during cooling are presented on the **Fig. 3**.

Charge material compositions were chosen in order to obtain compositions of sinters. Total number of experimental charges was 45. The results of samples stabilization depending on correlation of charge components are [resented on the **Fig. 4**.

The samples of charge material composition, which are located above the boundary line AB, are scattering during cooling. The boundary line, directed to the side of Al_2O_3–Ca_2SiO_4, testifies about the fact that increase of alumina amount in stable sinter leads to increase of the relation $Ca_2SiO_4/CaFe_2O_4+Al_2O_3$ and $Ca_2SiO_4/Ca_2Fe_2O_5+Al_2O_3$. At the same time increase of aluminium oxide amount up to 33-35 % allows to obtain stable sinters, and maximal content of dicalcium silicate in charge material reaches in this case 60 %.

The boundary of sinters stability is located along the line which is close to helenite in molar relation (Ca_2SiO_4/Al_2O_3=1). As it was shown on the Fig. 4*a*, ferrite, alumoferrite, helenite, two modifications of dicalcium silicate (β и γ) etc. were revealed in scattering sinters of the system $Ca_2Fe_2O_5$–Ca_2SiO_4–Al_2O_3 with alumina content up to 10 % (above the line AB) [31-33].

Small amount of β–Ca_2SiO_4 in the form of fine eutectic grains and overwhelming mass of γ–Ca_2SiO_4 in the form of more coarse and large grains with irregular form are presented as small prismatic crystals. Stable samples below the line AB (Fig. 4*b*) are characterized by overwhelming mass of β–Ca_2SiO_4 and small amount of γ–Ca_2SiO_4 inclusions.

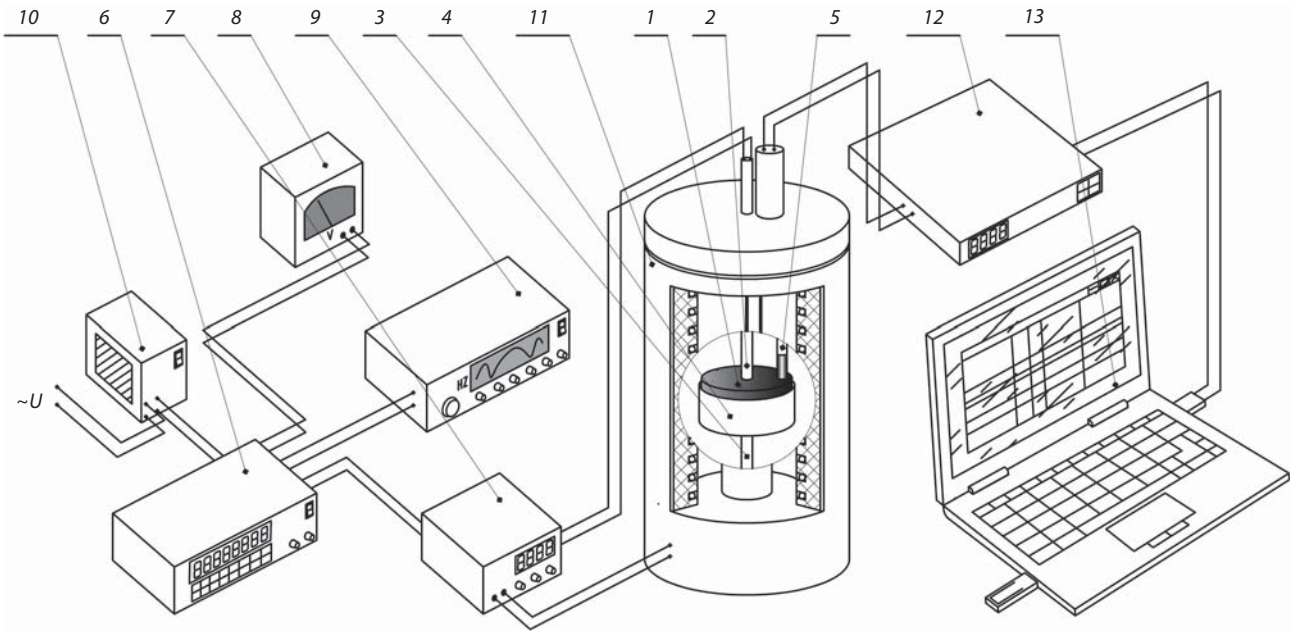

Fig. 2. The scheme of high-frequency unit with the high-temperature measuring cell:
1 – briquette; *2* – upper electrode; *3* – lower electrode; *4* – cup; *5* – thermocouple; *6* – generator; *7* – amplifier; *8* – voltmeter; *9* – frequency meter; *10* – power supply module; *11* – heating; *12* – control unit; *13* – data processing device

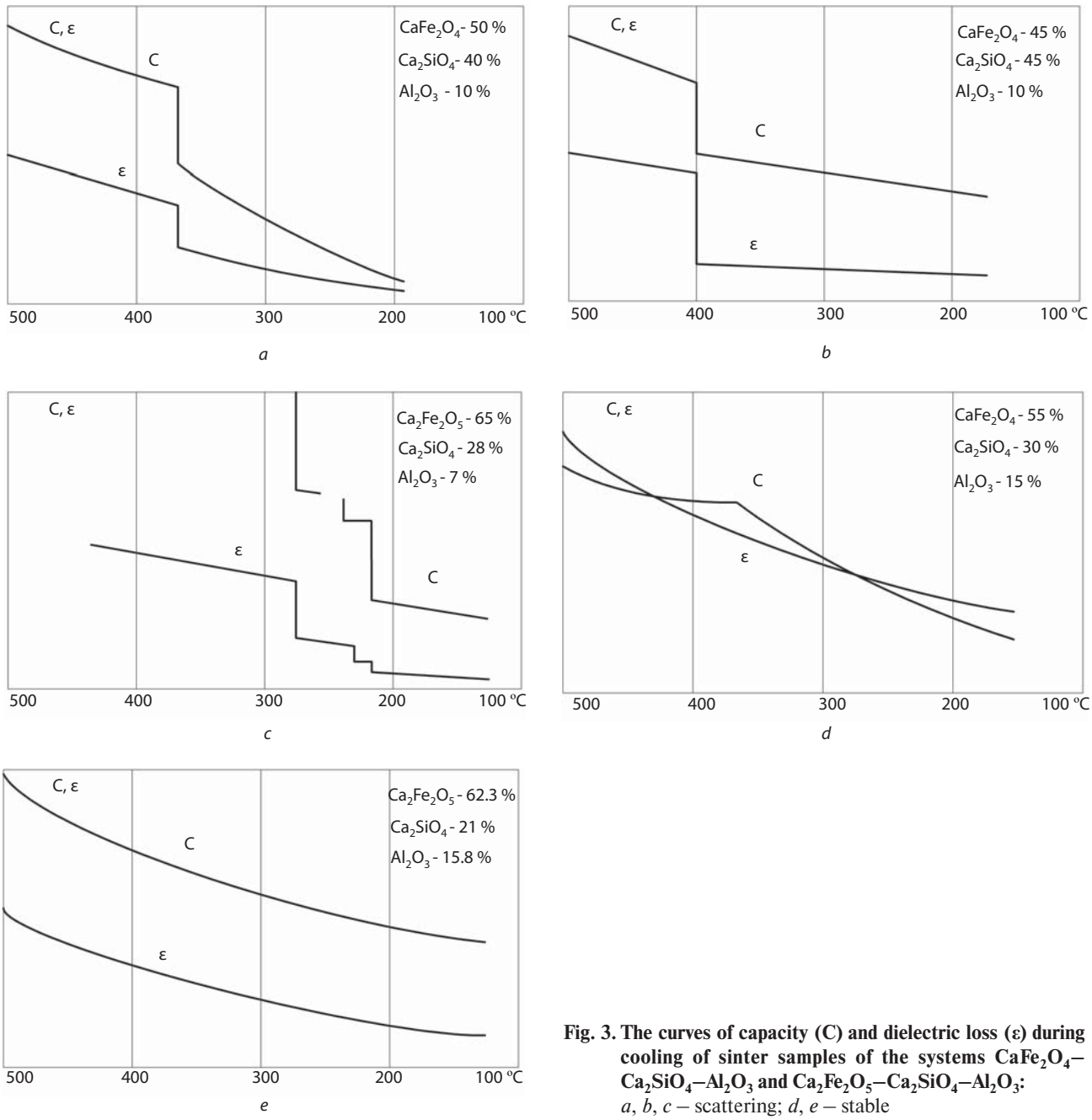

Fig. 3. The curves of capacity (C) and dielectric loss (ε) during cooling of sinter samples of the systems $CaFe_2O_4$–Ca_2SiO_4–Al_2O_3 and $Ca_2Fe_2O_5$–Ca_2SiO_4–Al_2O_3:
a, *b*, *c* – scattering; *d*, *e* – stable

Stable samples practically don't have silicate and very small amount of β–Ca_2SiO_4, but amount of helenite and alumoferrite increases apparently. The sinter with composition 63 % Ca_2SiO_4 and 37 % Al_2O_3 contains pure helenite.

It should be mentioned that obtaining of high-strength sinter in the system $Ca_2Fe_2O_5$–Ca_2SiO_4–Al_2O_2 requires rather more amount of aluminium oxide, than it was necessary for helenite forming, because part of aluminium oxide interacts with dicalcium ferrite with forming of solid solutions of helenite and brownmillerite. It is explained by complete Fe replacement by Al in dicalcium ferrite [34, 35].

The sinters which are located on the side of compositions $2CaO{\cdot}Fe_2O_3$–$2CaO{\cdot}SiO_2$, don't scatter, if amount of dicalcium silicate in these sinters does not exceed 5 %. Dicalcium silicate in these sinters is presented in the form of β–phase.

Results and discussion

Thus, the conducted tests display that ferrite can stabilize essentially less amount of dicalcium silicate (5 %) in the conditions of wide melt development, in comparison with sintering at the softening temperature (25 %).

It can be explained by transition of dicalcium silicate in the area of primary crystallization; this transition supports silicate decomposition during consequent sinter cooling due to large opportunities for grains enlargement up to critical size.

Maximal amount of dicalcium silicate in charge material, when sinters don't destroy in both cases, corresponds to the composition which is located on the straight line Ca_2SiO_4–Al_2O_3. It is connected with the fact that monocalcium ferrite does not form new compounds with

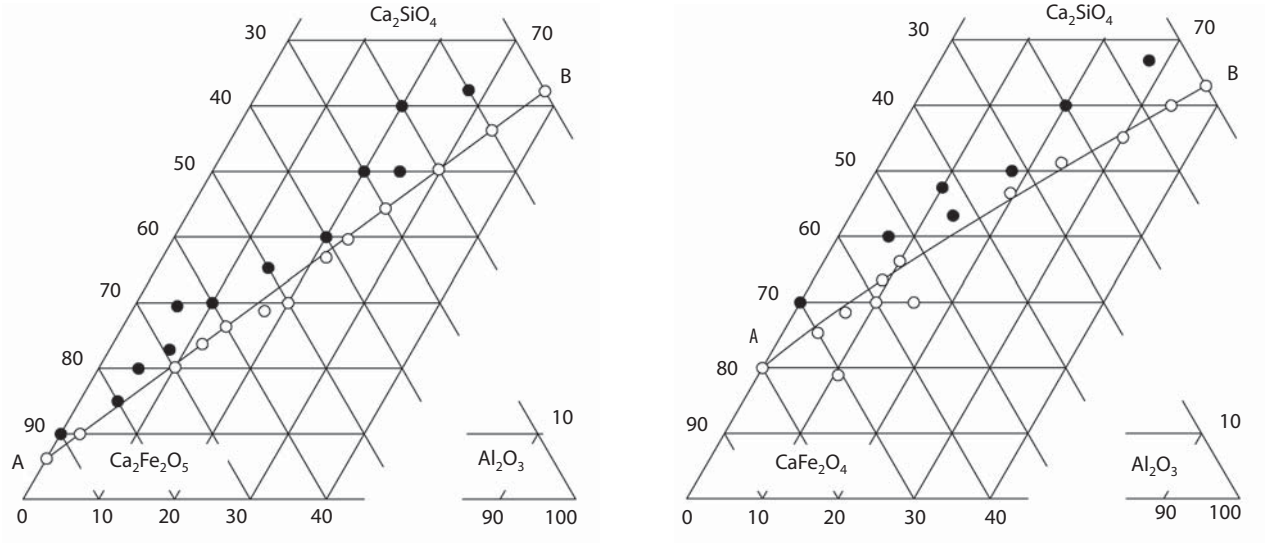

a *b*

Fig. 4. Diagrams of stable (white) and self-scattering sinters (black) in the systems:
a - $Ca_2Fe_2O_5$–Ca_2SiO_4–Al_2O_3; *b* - $CaFe_2O_4$–Ca_2SiO_4–Al_2O_3

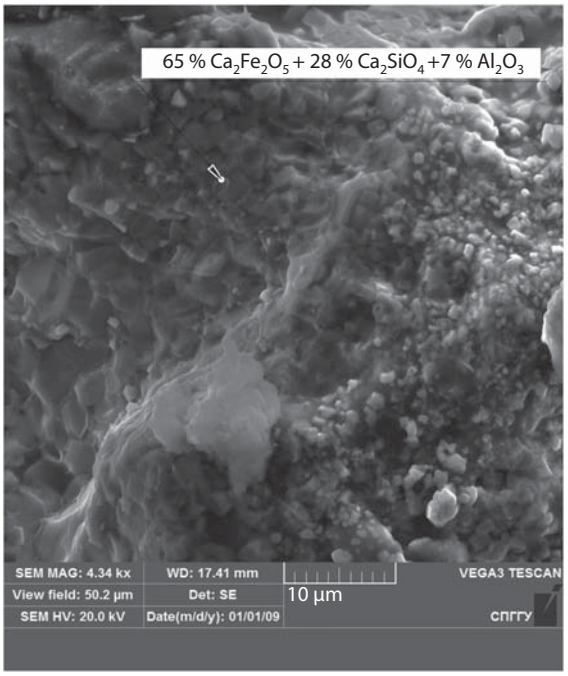

a

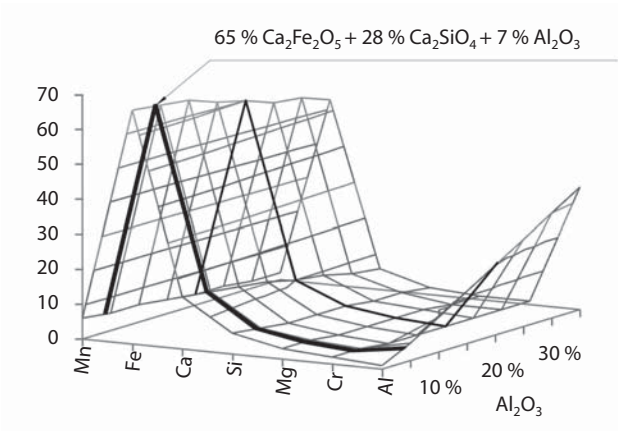

b

Fig. 5. Morphology (*a*) and chemical composition (*b*) of iron ore concentrate containing 7 % Al_2O_3 and 28 % Ca_2SiO_4
[these results were obtained by the authors]

aluminium oxide, which interacts completely with dicalcium silicate.

Cementation by monocalcium ferrite can be observed by microscope in the stable samples of the system $CaFe_2O_4$–Ca_2SiO_4–Al_2O_3 (**Fig. 5*a***). Amounts of alumosilicate and dicalcium silicate increase and decrease respectively with enlargement of alumina content.

Scattering samples are characterized by the breakpoint on the curve of dielectric losses during transition of dicalcium silicate in combination with a jump on the capacity curve. Such jump reflects the process of variation of physical structure in a destroying briquette. In this case the distinctly noted capacity variation by temperature and time coincides with variation of dielectric losses. The temperature of sample destruction is rather lower than that for a pure substance.

Stable sinters with complete binding of dicalcium silicate by aluminium oxide are characterized by monotonous variation of dielectric losses and capacity.

Analysis of the obtained curves shows that transition temperature depends also on composition of the samples. For $CaFe_2O_4$ – 50 %, Ca_2SiO_4 – 40 % and Al_2O_3 – 10 % a

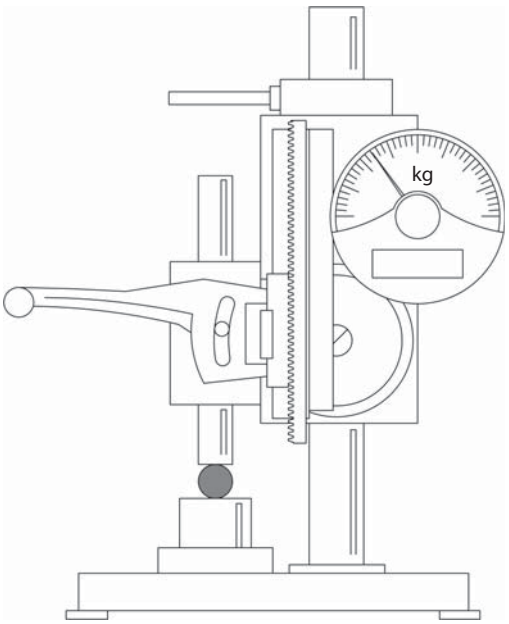

a

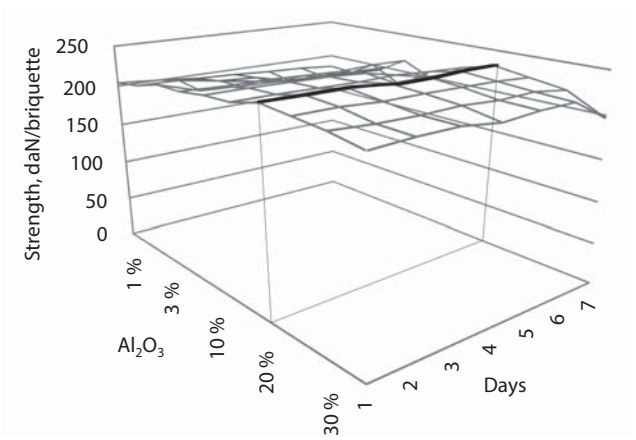

b

Fig. 6. Cold strength testing of iron ore concentrate containing 15 % Ca_2SiO_4 during 7 days
[these results were obtained by the authors]

jump on variation curves of electric properties corresponds to the temperature 370–385 °C; for $CaFe_2O_4$ – 45 % Ca_2SiO_4 – 45 %, Al_2O_3 – 10 % – it corresponds to the temperature 390–405 °C. As for the composition with dicalcium ferrite $Ca_2Fe_2O_5$ – 65 % , Ca_2SiO_4 – 28 %, Al_2O_3 – 7 %, this transition corresponds to the temperature 265–275 °C (Fig. 5*b*).

Assessment of quality variation in obtained sinters was determined via the technique similar to the GOST 24765-81 (briquette was compressed in axial / radial direction). Compression strength of briquette, which was mounted on generatrix, makes about 215-235 daN per briquette. The testing scheme for cold strength of a sintered briquette is presented on the **Fig. 6**.

If we shall compare the diagrams, the point A on the Fig. 4*b* is located rather higher than that on the Fig. 4*a*. Monocalcium ferrite has higher mechanical strength (by 15 %) in comparison with dicalcium ferrite, and it is capable to stabilize more amount of dicalcium silixcate. In this connection, the following correlation is valid for charge material of stable sinter: $Ca_2SiO_4/CaFe_2O_4 > Ca_2SiO_4/Ca_2Fe_2O_5$.

Agglomerate with basicity 1.3-1.5 practically does not contain free calcium oxide. Influence of silicon module becomes slight, i.e. free calcium is connected with alumina. The effect of aluminium module (CaO/Al_2O_3) replaces destructive effect of silicon module, what does not support appearance of stresses inside sinter. It is characterizes by increased mechanical strength (up to 225 daN per briquette) and resistance to destruction during long-term stacking in the conditions of increased humidity.

When adding aluminium oxide (up to 7 %), ortho-silicate decomposition of sinter is prevented, then strength decreases due to lowering of total Fe amount.

From the point of view of practical use, the obtained results can be useful for development of charge composition of fluxed agglomerate, providing its high strength; it also allows to improve commercial properties of blast furnace slags, which are used in building industry.

Conclusions

1. Dicalcium ferrite can stabilize up to 5 % dicalcium silicate.

2. Monocalcium ferrite does not form new compounds with aluminium oxide, which interacts completely with dicalcium silicate.

3. Stable samples of $CaFe_2O_4$–Ca_2SiO_4–Al_2O_3 system are characterized by cementation by monocalcium ferrite with increase of alumosilicate amount and decrease of dicalcium silicate amount.

4. Monotonous variation of dielectric losses and capacity occur for stable sinters, with complete binding of dicalcium silicate by aluminium oxide.

5. Transition temperature depends also on composition of samples. So, if Ca_2SiO_4 content decreases from 45 % to 28 %, the temperature lowers from 390–405 °C to 265–275 °C.

6. Briquette strength increases by 10 %, due to stabilization of larger amount of dicalcium silicate, what reduces stresses inside a sample.

7. Agglomerate with 7 % alumina content practically does not contain free calcium oxide and is characterized by high mechanic strength and resistance to destruction (up to 225 daN per briquette) during long-term stacking in the conditions of increased humidity.

8. Adding of aluminium oxide up to 7 % prevents ortho-silicate sinter decomposition, then strength decreases due to lowering of total Fe amount.

REFERENCES

1. Frolov Yu. A. Sintering. Technology. Heat engineering. Management. Ecology. Moscow : Metallurgizdat. 2016. 672 p.
2. Bersenev I. S., Petryshev A. Yu., Kolyasnikov A. Yu., Milokhin E. A., Semenov O. A., Isaenko G. E. Improving the Sinter at PAO NLMK. *Steel in Translation*. 2018. Vol. 48. No. 9. pp. 585–592.
3. Bersenev I. S., Gorbachev V. A., Klein V. I., Petryshev A. Yu., Yaroshenko Yu. G. To the problem of connection between ultimate stresses in agglomerate and its strength in rotating drum. *Stal*. 2013. No. 1. pp. 6-8.
4. Bobkov V. I., Dli M. I., Fedulov A. S. Imitating simulation of the drying process of sinters from wastes of apatite-nepheline ores. *Izvestiya Sankt-Peterburgskogo gosudarstvennogo tekhnologicheskogo institute (tekhnicheskogo universiteta)*. 2020. No. 55. pp. 109-115.
5. Su Z., Li L., Liu Z., Huang C., Wang D., Wang T. Fabrication, microstructure, and hydration of nano β-Ca_2SiO_4 powder by co-precipitation method. *Construction and Building Materials*. 2021. Vol. 296. p. 123737. DOI: 10.1016/j.conbuildmat.2021.123737.
6. Cheng S., Shevchenko M., Hayes P.C. , Jak E. Experimental Phase Equilibria Studies in the FeO-Fe_2O_3-CaO-SiO_2 System in Air: Results for the Iron-Rich Region. *Metallurgical and Materials Transactions B*. 2020. Vol. 51.No. 4. pp. 1587–1602.
7. Malysheva T. Ya., Dolitskaya O. A. Petrography and mineralogy of iron ore raw materials. A manual for high schools. Moscow : MISiS. 2004. 424 p.
8. Puzanov V. P., Kobelev V. A. Introduction in the technologies of metallurgical structure forming. Ekaterinburg : UrO RAN. 2005. 501 p.
9. Nechkin G. A. Study of the influence of mineral structure forming on metallurgical properties of iron ore agglomerates. Dissertation... of a Candidate of Technical Sciences. Institute of Metallurgy of the Ural branch of RAS. Ekaterinburg. 2015. 141 p.
10. Efimenko G. G., Kovalev D. A. Management of the process of agglomerate structure forming for its strengthening. *Izvestiya AN SSSR. Metally*. 1966. No. 6. pp. 3-10.
11. Jin J , Liu X. , Yuan S., Gao P., Li Y., Zhang H., Meng X. Innovative utilization of red mud through co-roasting with coal gangue for separation of iron and aluminum minerals. *Journal of Industrial & Engineering Chemistry*. 2021. Vol. 98. pp. 298–307. DOI: 10.1016/j.jiec.2021.03.038.
12. Grudinskii P. I., Dyubanov V. G., Zinoveev D. V., Zheleznyi M. V. Solid-Phase Reduction and Iron Grain Growth in Red Mud in the Presence of Alkali Metal Salts. *Russian Metallurgy (Metally)*. 2018. No. 11. pp. 1020–1026. DOI: 10.1134/S0036029518110071.
13. Korzhaeva E. E., Voishchev A. E., Khoshafyan S. O., Bataeva F. A., Buntov V. V., Iskanderov R. D. Study of the effect of receipt parameters on forming a joint structure and properties of heavy concrete. *Vestnik Evraziyskoy nauki*. 2019. Vol. 11. No. 6. p. 9.
14. Kudinova A. A., Poltoratckaya M. E., Gabdulkhakov R. R., Litvinova T. E. , Rudko V. A. Parameters influence establishment of the petroleum coke genesis on the structure and properties of a highly porous carbon material obtained by activation of KOH. *Journal of Porous Materials*. 2022. Vol. 11. No. 6. p. 9.
15. Mardashov D. V., Bondarenko A. V., Raupov I. R. Design procedure of technological parameters of non-Newtonian fluids injection into an oil well during workover operation. *Journal of Mining Institute*. 2022. DOI: 10.31897/PMI.2022.16.
16. Pavlovets V. M. Use of pore-forming additives of plant origination in manufacture of iron-containing agglomerated raw material. *Vestnik Sibirskogo gosudarstvennogo industrialnogo universiteta*. 2019. No. 3 (29). pp. 14-20.
17. Trushko V. L., Utkov V. A., Bazhin V. Y. Topicality and Possibilities for complete processing of red mud of aluminous production. *Journal of Mining Institute*. 2017. Vol. 227. pp. 41–47.
18. Polyakov A., Gorlanov E. , Mushihin E. Analytical Modeling of Current and Potential Distribution over Carbon and Low-Consumable Anodes during Aluminum Reduction Process. *Journal of The Electrochemical Society*. 2022. Vol. 169. DOI: 10.1149/1945-7111/ac6a16.
19. Zubkova O. S., Alexeev A. I., Sizyakov V. M., Polyanskiy A. S., Research of suxfuric acid salts influence on sedimentation process of a clay suspension. *ChemChemTech*. 2022. Vol. 65. No. 1. pp. 44–49. DOI: 10.6060/ivkkt.20226501.6447.
20. Khalifa A., Bazhin V., Kuskova Y., Abdelrahim A., Ahmed Y. Study the Recycling of Red Mud in Iron Ore Sintering Process. *Journal of Ecological Engineering*. 2021. Vol. 22. No. 6. pp. 191–201. DOI: 10.12911/22998993/137966..
21. Shao F., Zhuang Y., Ni J., Sheng J., Zhao H., Tao S., Yang K. Comparison of the microstructural characteristics and electrical properties of plasma sprayed Al_2O_3 and Al_2O_3–Ca_2SiO_4 coatings immersed in deionized water. *Surface and Coatings Technology*. 2021. Vol. 422. p. 127530. DOI: 10.1016/j.surfcoat.2021.127530.
22. Karpova K. S., Karpov A. V. Solid phase reduction of iron oxides in laboratorial conditions. *Sovremennye materialy, tekhnika i tekhnologii*. 2018. No. 1 (16). pp. 27–32.
23. Krylova S. A., Sysoev V. I., Alekseev D. I., Sergeev D. S., Dudchuk I. A. Physical-chemical parameters of high-magnesial siderites. *Vestnik Yuzhno-Uralskogo gosudarstvennogo universiteta, Seriya: Metallurgiya*. 2017. Vol. 17. No. 2. pp. 13-21.
24. Ortega J. M., Cabeza M., Tenza-Abril A. J., Real-Herraiz T., Climent M. Á., Sánchez I. Effects of Red Mud Addition in the Microstructure, Durability and Mechanical Performance of Cement Mortars. *Applied Sciences*. 2019. Vol. 9. No. 5. p. 984. DOI: 10.3390/app9050984.
25. Boikov A. V., Savelev R. V., Payor V. A., Erokhina O. O. The control method concept of bulk material behaviour in the pelletizing drum for improving the results of DEM-modeling. *CIS Iron and Steel Review*. 2019. Vol. 17. pp. 10–13.
26. Omelchenko I. N., Kuznetsov A. A. New tendencies on the iron ore market. *Gumanitarnyi vestnik*. 2017. No. 8 (58). p. 7.
27. Maksimov L. I., Mironov V. V. Improvement of manufacturing technology for metallic iron powders from a sediment of deferrization station. *Vestnik Tomskogo gosudarstvennogo arkhitekturno-stroitelnogo universiteta*. 2020. Vol. 22. No. 2. pp. 162–173.
28. Aydin S., Aydin M. E., Beduk F., Ulvi A. Removal of antibiotics from aqueous solution by using magnetic Fe3O4/red mud-nanoparticles. *Science of The Total Environment*. 2019. Vol. 670. pp. 539–546. DOI: 10.1016/j.scitotenv.2019.03.205.
29. Hoang M. D., Do Q. M., Le V. Q. Effect of curing regime on properties of red mud based alkali activated materials. *Construction and Building Materials*. 2020. Vol. 259. p. 119779. DOI: 10.1016/j.conbuildmat.2020.119779.
30. Trushko V. L., Utkov V. A. Development of import subtituting technologies for increasing productivity of sintering machines and strength of agglomerates. *Journal of Mining Institute*. 2016. No. 221. p. 675. DOI: 10.18454/pmi.2016.5.675.
31. Shiryaeva E. V., Podgorodetskiy G. S., Malysheva T. Ya., Detkova T. V., Gorbunov V. B. Influence of low-alkali red mud on composition and structure of agglomeration charge material made of iron ore concentrates with different genesis. *Izvestiya vysshikh uchebnykh zavedeniy. Chernaya metallurgiya*. 2015. Vol. 57. No. 9. pp. 13–17. DOI: 10.17073/0368-0797-2014-9-13-17.
32. Sizyakov V. M., Brichkin V. N. On the role of calcium hydrocarboaluminates in improvement of the technology of complex processing of nephelines. *Zapiski Gornogo instituta*. 2018. Vol. 231. pp. 292–298. DOI: 10.25515/PMI.2018.3.292.
33. Aleksandrov V. I., Vasilyeva M. A. Hydrotransport for condensed tailings of iron ore concentration at Kachkanarskiy GOK based on the results of pilot-industrial tests of hydraulic transport system. *Zapiski Gornogo instituta*. 2018. Vol. 233. pp. 471-479. DOI: 10.31897/PMI.2018.5.471.
34. Sharikov Yu. V., Sharikov F. Yu., Titov O. V. Optimal control of annealing during the preparation of aluminum hydroxide and cement clinker in tubular rotary kilns. *Theoretical Foundations of Chemical Engineering*. 2017. Vol. 51. No. 4. pp. 503–507. DOI: 10.1134/S0040579517030125.
35. Bazhin V. Y., Khalifa A. A., Shalabi M. E. K. Study of the kinetics of the process of producing pellets from red mud in a hydrogen flow. *Journal of Mining Institute*. 2022. Vol. 254. pp. 261-270. DOI: 10.31897/PMI.2022.18.